Amination of polyethylene glycol to polyetheramine over the supported nickel catalysts

Jih-Mirn Jehng * and Chia-Ming Chen

Department of Chemical Engineering, National Chung Hsing University, Taichung 402, Taiwan, ROC
E-mail: jmjehng@dragon.nchu.edu.tw

Received 8 June 2001; accepted 8 August 2001

Surface nickel (NiO_x) species, surface $NiAl_xO_y$ compound, and NiO crystallites are present on the Ni/Al_2O_3 catalysts, and the ratio of these nickel species is dependent on the nickel loading. Surface nickel interacts with the TiO_2 support to form a surface nickel titanate compound ($NiTiO_x$) which has a lower reducibility. The weak interaction between the surface nickel and the silica support results in the formation of NiO crystallites on the SiO_2 surface. The Ni/Al_2O_3 and Ni/TiO_2 catalysts contain new surface Lewis acid sites and the amount of surface Lewis acid sites increases with increasing nickel concentration. The Ni/SiO_2 catalysts have no sign of the presence of the surface Lewis acid sites. Only the Ni/Al_2O_3 catalysts have shown the ammonia adsorption at temperature of 200 °C. Supported nickel on alumina catalysts possess the highest amination conversion, and the amine yield increases with increasing nickel loading up to ∼15% and starts to level off. By comparing amination catalysis with quantitatively TPR studies of the H_2 consumed of the Ni/Al_2O_3 catalysts, it appears that the dispersed nickel species are the active sites for amination. In addition, the amination product is mainly the secondary amine due to the presence of water.

KEY WORDS: supported nickel catalyst; reducibility; surface acidity; polyethylene glycol (PEG); amination

1. Introduction

Derivatives obtained from polyetherpolyamine have applications in various chemical industries including curing agents for epoxy resins, plasticizers, cross-linking agents for textiles, defoamers, and drug carriers for pharmaceutics [1–4]. Raney catalysts have been extensively used in the hydrogenation/dehydrogenation of hydrocarbons [5,6]. In the area of amination processes, a nickel-based catalyst (including Raney catalyst and nickel in combination with other metals or metal oxides) has been applied for the amination of polyethyleneglycol (PEG) and polypropyleneglycol (PPG) to form polyoxyalkylene polyamines [1–3].

Polyoxyalkylenediamines were prepared by reaction of polyoxyalkylene glycols with ammonia and hydrogen over a Raney catalyst [2]. One of the disadvantages of this process is the poor yield due to the use of the higher molecular weight polyoxyalkylene glycols and the unavailability of a particular way to remove the unreacted glycol from the desired diamines. The second disadvantage of this process is that the catalyst could be softened by the presence of water and ammonia under reaction conditions, and thus cause the breakdown of the operation due to the blocking of the reactor. An effective amination catalyst for preparing polyoxyalkylene polyamines was developed by Jefferson chemical company in order to obtain good yield [1]. In this modified process, polyoxyalkylene glycols were treated with ammonia and hydrogen at a temperature of 150–275 °C and a pressure of 500–5000 psig in a fixed-bed reactor over a mixed metal catalyst containing 60–85 mol% nickel, 14–37 mol% copper and 1–5 mol% chromium. The modified catalysts have improved the reducibility of the active metal component and the physical stability of the catalyst under reaction conditions. A less reducible catalyst has no physical stability under the amination process and is not suitable for a continuous process. The reduced metal in the nickel–copper–chromium catalyst, ranging from 30 to 90%, is a physically stable catalyst for the amination reaction [1].

The main object of this study is to develop a novel catalyst for the amination of PEG (or PPG) to polyetherpolyamine. Supported metal catalysts will be the preferred catalysts for the preparation of polyoxyalkylene polyamines, since the supported nickel catalyst has been effectively used in the amination of cyclohexanol to cyclohexylamine (Ni-5124 T 3/16″, Harshaw) [7–9]. In 1978, Tauster *et al.*'s studies [10–12] on the supported metal catalysts have revealed that the catalytic properties of a metal can be significantly changed by the presence of a strong metal–support interaction (SMSI). It appears that supports usually possess a high surface area, high thermal and chemical stability, and high mechanical strength, and are used as inert carriers of the active component. Consequently, the metal–support interactions will be used to molecularly design catalysts exhibiting high activity and selectivity for the amination process. As mentioned above, the polyetherpolyamine derivatives have various applications in specialty chemicals such as epoxy resins, polymer surfactants, anti-static agents, and drug carriers. Thus, the molecular design of a novel amination catalyst is essential for controlling the structures of the polyetherpolyamine derivatives and their applications, and the

* To whom correspondence should be addressed.

development of this catalytic technology should have a pronounced effect on the specialty chemical industry and provide more opportunities in the production of "performance chemicals".

2. Experimental

2.1. Materials and preparation

The Ni supported on TiO_2 (Degussa P-25, ∼50 m^2/g), Al_2O_3 (calcined $Al(OH)_3$ at 500 °C, ∼210 m^2/g), and SiO_2 (Cab-O-Sil, ∼300 m^2/g) catalysts were prepared by the incipient-wetness impregnation method. Nickel nitride (Alfa, ∼98% purity), dissolved in an appropriate amount of distilled water, was impregnated into the metal oxide support to form a wetted solid mixture. The mixture was initially dried at room temperature overnight to remove excess water and further dried at 120 °C for 1 h and 300 °C for 1 h. The sample was finally calcined at 500 °C for 2 h under a 30 cm^3/min flowing rate of air in order to form supported nickel catalysts. The supported nickel catalysts were prepared with nickel loading from 1 to 60 mol% on TiO_2, Al_2O_3, and SiO_2 oxide supports. The bonding between the surface metal and the oxide support was varied during the preparation step. The final state of surface metal was dependent on metal component, support, preparation method, calcined temperature and reduction condition [13,14].

2.2. BET surface area measurement

A high-performance volumetric physisoption apparatus (Micromeritics ASAP 2010) was used to determine the pore size distribution and BET surface area of the supported nickel catalysts. A 0.1–0.4 g of sample was first degassed with flowing 30 cm^3/min He gas to remove the impurities and water on the sample. Then, the nitrogen gas was introduced into the sample quartz tube to perform the adsorption of nitrogen under the liquid nitrogen temperature and calculate the surface area from the amount on nitrogen molecules adsorbed.

2.3. ESCA/XPS measurement

X-ray photoelectron spectroscopy (Physical Electronics, USA, PHI 1600) was used to obtain a chemical analysis of the surface from the assignment of the measured binding energies and the oxidation state of the surface metal species. The transition of a two-dimensional surface metal monolayer to a three-dimensional metal crystalline phase and the dispersion of the surface metal on the support can also be determined.

For different nickel loadings of Ni/SiO_2, Ni/TiO_2 and Ni/Al_2O_3 catalysts, $[Ni/M]_{surface}$ (M = Si, Ti or Al) ratios can be calculated from the ESCA/XPS experiments. The ratio of $[Ni/M]_{bulk}$ (M = Si, Ti or Al) can be obtained from calculating the bulk nickel concentration of the catalyst. Then, the $[Ni/M]_{surface}$ *vs.* $[Ni/M]_{bulk}$ plot can be used to analyze the surface dispersion of nickel on the metal oxide supports.

2.4. Temperature-programmed reduction (TPR)

A TPR system (Zeton–Altamira, AMI-100) was used to study the reducibility of the supported nickel catalysts as a function of oxide support and nickel loading. A 0.05–0.08 g sample was first treated to 500 °C with a 20 °C/min heating rate under flowing a 10% O_2/He mixture gas, and maintained at 500 °C for 1 h in order to remove the adsorbed moisture and oxidize the catalysts. The sample was then cooled down to room temperature and maintained at room temperature for 30 min. Then, the treatment gas was switched to 5% H_2/He mixture with a 10 °C/min heating rate to a final temperature of 800 °C. The consumption of H_2 molecules per weight of catalyst upon reduction experiment was analyzed and measured by AMI-100's integration package.

2.5. Surface acidity studies

Chemisorption of pyridine and ammonia followed by FTIR studies is usually a useful probe for investigating the presence and nature of surface Lewis acid and Brønsted acid sites on a catalyst surface. According to Knözinger, the vibrational modes of pyridine that are the most affected through such intermolecular interactions are the ring-stretching modes (originally at 1439 and 1583 cm^{-1}, respectively) [15]. Pyridine coordinatively bonded to Lewis acid sites (PyL) was observed at 1450, 1490, 1580 and 1600 cm^{-1}, and the most strong intensity appears at 1450 cm^{-1}. Pyridinium ions (PyH^+) bonded to Brønsted acid sites are observed at 1490, 1540, 1620 and 1640 cm^{-1}. About the adsorption of NH_3, the peaks of Lewis and Brønsted acid sites are observed at about 1600 and 1455 cm^{-1}, respectively.

The IR spectra of the supported nickel catalysts were recorded on a FTIR (Perkin–Elmer Paragon 500) spectrometer with a resolution better than 4 cm^{-1}. The sample was pressed into a 13 mm self-supported disc and placed into an *in situ* IR cell. The cell was heated at 500 °C under flowing dry air for 1 h to oxidize the catalyst, and then cooled down to 200 °C. Upon evacuating the cell to 10^{-4} Torr, the IR spectrum of the sample before adsorption was recorded. Pyridine was then introduced into the cell at 30 Torr (for ammonia at 60–70 Torr) and contacted with the catalyst for 15 min. Physically adsorbed pyridine can be subsequently desorbed by maintaining the sample in vacuum for 30 min, and the IR pyridine adsorption spectrum was recorded again.

2.6. Amination studies

A known amount of PEG-400 with ∼30 wt% of ammonia solution was loaded into a 600 cm^3 autoclave (Parr, model 4563). A 5 g of supported nickel catalyst was also added into the reactor. It was ensured that all the valves and screws on the reactor were closed and tightened. The reactor was then pressurized by nitrogen gas to ∼2 bar and released to atmospheric pressure. The last step was repeated for three times in order to purge out the air in the reactor. After the

purging steps, hydrogen gas was introduced into the reactor till the reactor pressure has reached ∼9 bar. Finally, the total pressure of the reactor was increased to ∼34 bar by introducing nitrogen gas. The amination reaction was performed at a temperature between 150 and 250 °C, and samples were collected at 30 min reaction intervals. The collected samples were analyzed by a titration method to calculate the total amine yield and the order of amine products.

3. Results and discussion

Characterization of the supported metal phase is essential to establish a relationship between metal structure and performance. The catalytic properties of the catalyst can be optimized by manipulating its structure and composition. Thus, the establishment of a structure–function relationship of the supported metal catalysts provides additional knowledge in the catalyst design. Basically, many techniques can be used for characterizing the supported metal phase such as chemisorption, X-ray diffraction and X-ray photoelectron spectroscopy, electron microscopy, and then study of the catalytic properties [15–22]. The objective of the characterization method is to shed light onto the physical and chemical properties (such as dispersion, surface area, particle size and oxidation state) of the catalysts. Schwab *et al.* have shown that the interaction between metal and oxide support of the Ni/Al_2O_3, Co/Al_2O_3, and Ag/Al_2O_3 catalysts strongly affects the catalytic properties of formic acid dehydrogenation [23,24].

3.1. BET surface area

BET measurements of the supported nickel catalysts (see figure 1) have shown that the surface area decreases slowly with increasing nickel loading and no mixed bulk oxide crystals are present, which usually possess very low surface area. It appears that nickel metal forms a surface layer covering the oxide supports and maintains the available surface area. The dispersion of the surface nickel phase will be further determined by the ESCA/XPS studies in the following section. The presence of the surface nickel layer will strongly affect the reactivity and reducibility of the supported metal catalysts.

3.2. ESCA/XPS

The results of ESCA/XPS measurements are shown in figure 2. The $[Ni/Al]_{surface}$ ratio of the Ni/Al_2O_3 catalysts was increased with the increasing of nickel loading. Up to 3% nickel loading, the $[Ni/Al]_{surface}$ ratio is linearly increased with increasing of the $[Ni/Al]_{bulk}$ ratio. Above 3% nickel loading, the $[Ni/Al]_{surface}$ ratio slightly deviates from the linear relation with further increasing of the $[Ni/Al]_{bulk}$ ratio. For the Ni/TiO_2 and Ni/SiO_2 catalysts, the $[Ni/M]_{surface}$ ratio (M = Ti or Si) is linearly increased with $[Ni/M]_{bulk}$ (M = Ti or Si) ratio only up to ∼1% nickel loading due to the formation of larger nickel particles or crystalline NiO. It appears that the dispersion of surface nickel species on the Al_2O_3 support is higher than on the TiO_2 and SiO_2 supports. Surface nickel oxide on TiO_2 and SiO_2 supports may form a surface nickel oxide compound or crystallite of nickel metal oxide which results in the lower dispersion of nickel oxide on the surface.

3.3. TPR experiments

During the process of amination reaction, the reducibility of the supported metal oxide can be used as an important characteristic to evaluate the performance of an effective catalyst. The bonding between surface nickel phase and supports strongly affects the reducibility of catalysts. From the results of TPR experiments, the reduction temperatures of surface nickel oxide on SiO_2 for different nickel loading levels were between 275 and 320 °C, 359 and 384 °C, and 430 and 465 °C. The reduction temperatures were slightly increased with nickel loading, as shown in figure 3, or no change was obtained. Below a 3% nickel loading, the highest reduction temperature of surface nickel oxide on the TiO_2 support was between 450 and 465 °C, as shown in figure 4, and the reduction temperatures were shifted to 400 °C and 495–500 °C with increasing nickel loading above 3%, as shown in figure 4. On the Al_2O_3 support, the reduction

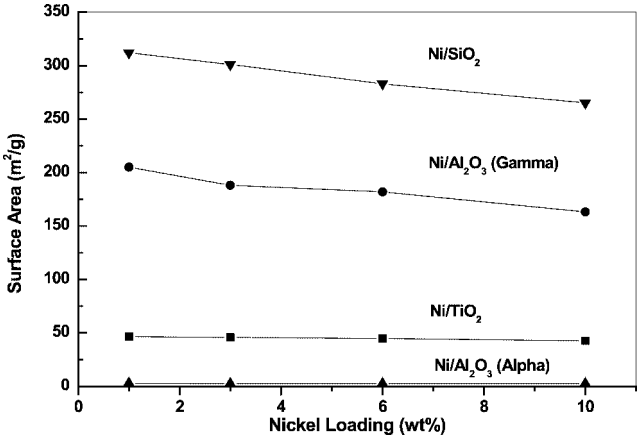

Figure 1. Surface area of supported nickel oxide catalysts.

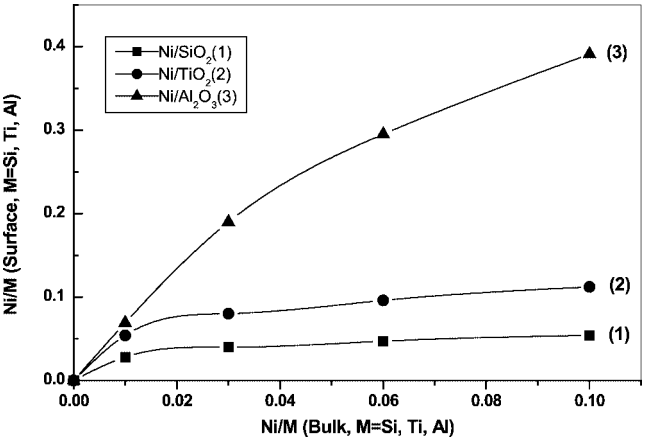

Figure 2. XPS studies of supported nickel catalysts.

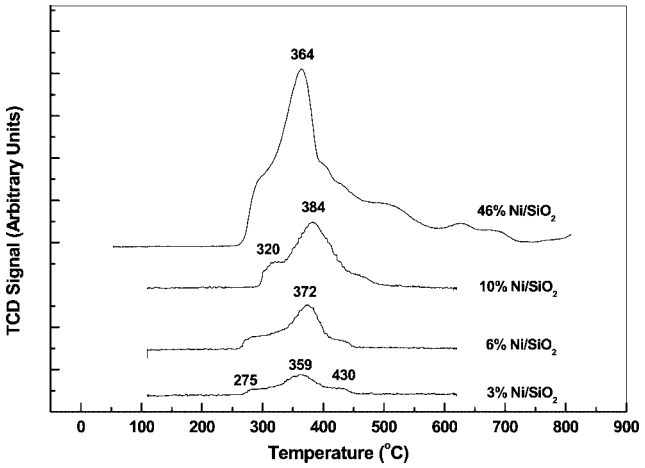

Figure 3. TPR studies of supported nickel on SiO_2 as a function of nickel loading.

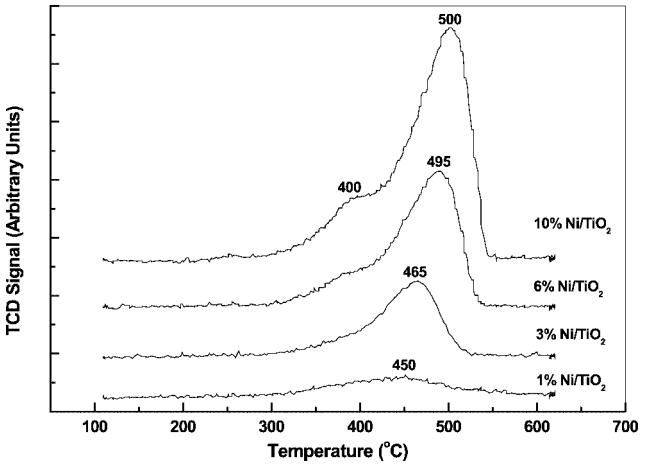

Figure 4. TPR studies of supported nickel on TiO_2 as a function of nickel loading.

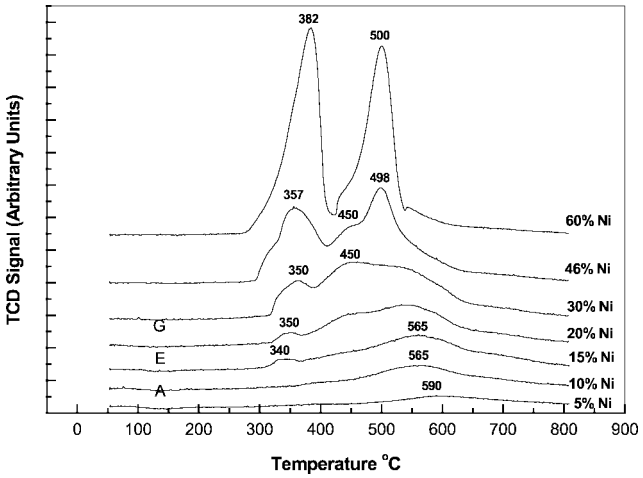

Figure 5. TPR studies of supported nickel on Al_2O_3 as a function of nickel loading.

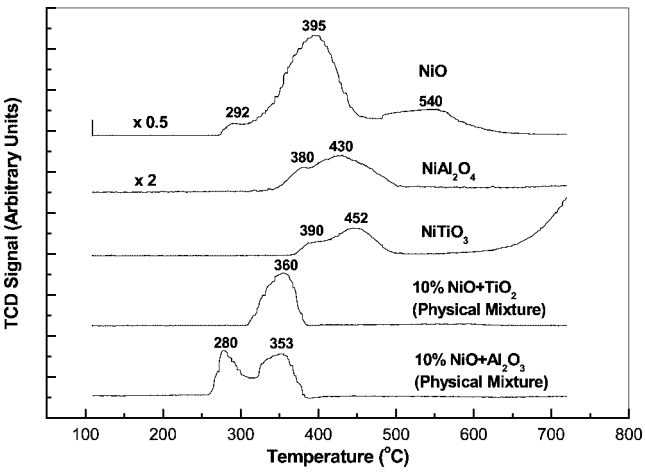

Figure 6. TPR studies of nickel reference compounds.

temperature between 565 and 590 °C appears at the nickel loading below ∼15%. The reduction peaks were gradually increased with increasing nickel loading, as shown in figure 5. As the nickel loading was increased above 15%, multiple reduction peaks appear between 350 and 382 °C, and 450 and 500 °C. This indicates that different surface nickel species are present on the Al_2O_3 support. Comparing the results of TPR experiments in figures 3–5 with the reference nickel compound of TPR in figure 6, it appears that different structures of surface nickel oxide may appear on different supports.

The reduction peaks of Ni/SiO_2 in figure 3 are similar to those of NiO crystallites in figure 6. TPR results indicates that nickel metal forms crystals of NiO on SiO_2. This is consistent with the results of previous ESCA/XPS experiments. The surface characteristics of SiO_2, which is less hydrophobic and has fewer OH groups than the other supports, can restrain the metal and metal oxide to form a surface overlayer and results in a lower dispersion. The reduction peaks of Ni/TiO_2 as shown in figure 4, are similar to those of $NiTiO_3$ in figure 6 that has two different peaks between 390 and 500 °C. However, the Ni/TiO_2 catalyst does not have a reduction peak at 800 °C. This suggests that nickel metal react with TiO_2 to form a non-stoichiometric $NiTiO_x$ compound on the surface. The Ni–Ti–O bonds in the $NiTiO_x$ compound can maintain the stability of the catalyst under reaction conditions [25]. The reduction peaks of Ni/Al_2O_3 with higher nickel loading in figure 5 are similar to the combination reduction features of $NiAl_2O_4$ and NiO reference compounds in figure 6. TPR studies of the Ni/Al_2O_3 catalysts with nickel loading below ∼15% indicate that nickel metal forms surface nickel species on the Al_2O_3 surface possessing a reduction peak at 560–590 °C which is different from any reduction peaks shown in the reference compounds (figure 6).

In addition, the H_2 consumption of the Ni/Al_2O_3 catalysts increases with increasing the nickel loading up to ∼15% and starts to level off with further increasing nickel loading (see figure 7). The presence of a high concentration of surface nickel species on Al_2O_3 required more hydrogen to perform the reduction. The reducibility of the supported nickel catalyst depends on the surface nickel–support interaction and

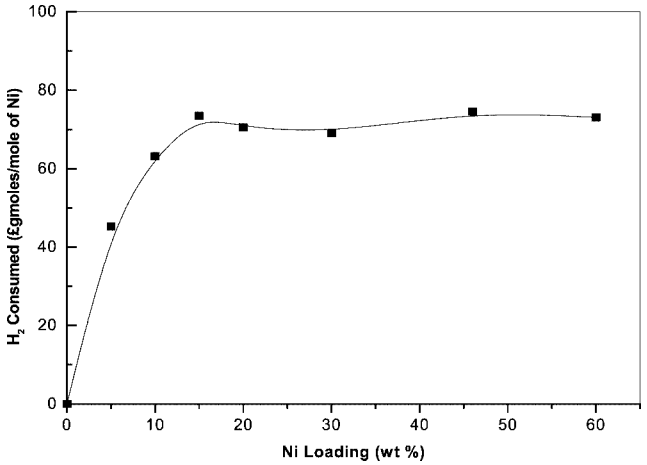

Figure 7. H_2 consumption of the Ni/Al_2O_3 catalysts.

its surface structure. The surface nickel species on oxide support are more difficult to reduce than nickel oxide crystallites. Thus, the structural properties of the surface metal or metal oxide can affect the reducibility of the catalyst.

3.4. Surface acidity studies

Surface acidity of supported metal or metal oxide catalysts can be analyzed by IR spectroscopy of pyridine adsorption. For pyridine adsorption, IR peaks appearing at 1450, 1490, 1580 and 1600 cm^{-1} are characteristic for pyridine coordinatively bonded to Lewis acid sites (PyL); the strongest intensity appears at 1450 cm^{-1}. IR peaks appearing at 1490, 1540, 1620 and 1640 cm^{-1} are characteristic for pyridinium ion (PyH^+). Thus the pyridine adsorption can qualitatively and quantitatively analyze the presence of the Lewis and Brønsted acid sites on the catalyst's surface.

It appears that the SiO_2 support does not contain any acid sites on the surface [26]. From the previous XPS and TPR studies, the weak interactions between nickel atom and silica result in the formation of a crystalline or microcrystalline phase of NiO on the silica surface. The deposition of nickel metal does not form a surface nickel overlayer on silica, and pyridine adsorption does not occur on the Ni/SiO_2 catalysts. The TiO_2 support has some weak Lewis acid sites [26]. The deposition of nickel atoms on TiO_2 replaces weak Ti Lewis acid sites by the slightly stronger Ni Lewis acid sites (the frequency of PyL band remains at 1445 cm^{-1}). The increase of the PyL band intensity with increasing nickel loading (figure 8) suggests that the Ni deposition creates more coordinatively unsaturated sites. Combining with the previous structural information, the formation of a surface $NiTiO_x$ compound on the Ni/TiO_2 catalysts can be responsible for the increase of surface Lewis acid sites. The IR spectra of pyridine adsorbed on Ni/Al_2O_3 catalysts are presented in figure 9. The Al_2O_3 support does not contain surface Brønsted acid sites, but contains strong surface Lewis acid sites (PyL band at $\sim$1450 cm^{-1}). The addition of nickel to the Al_2O_3 surface affects the characteristics of the surface Lewis acid sites. The PyL band intensity increases with nickel loading

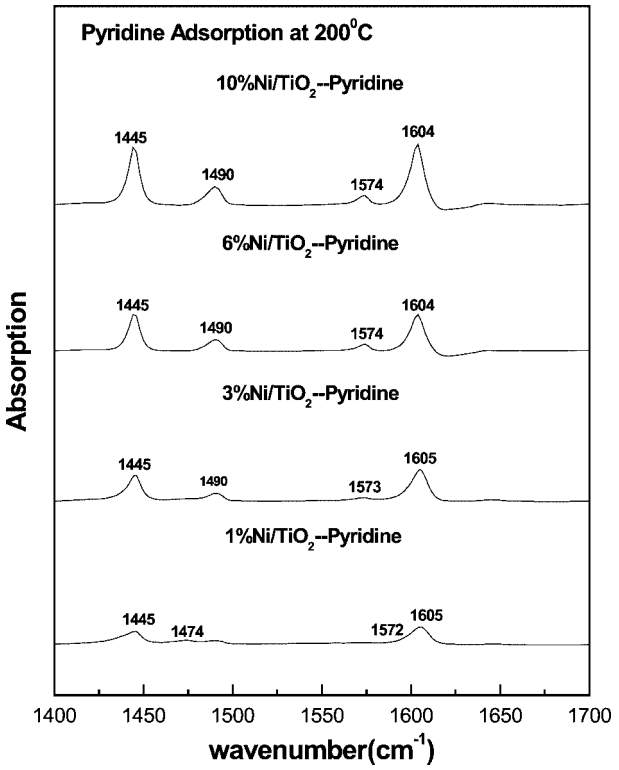

Figure 8. Pyridine adsorption on Ni/TiO_2.

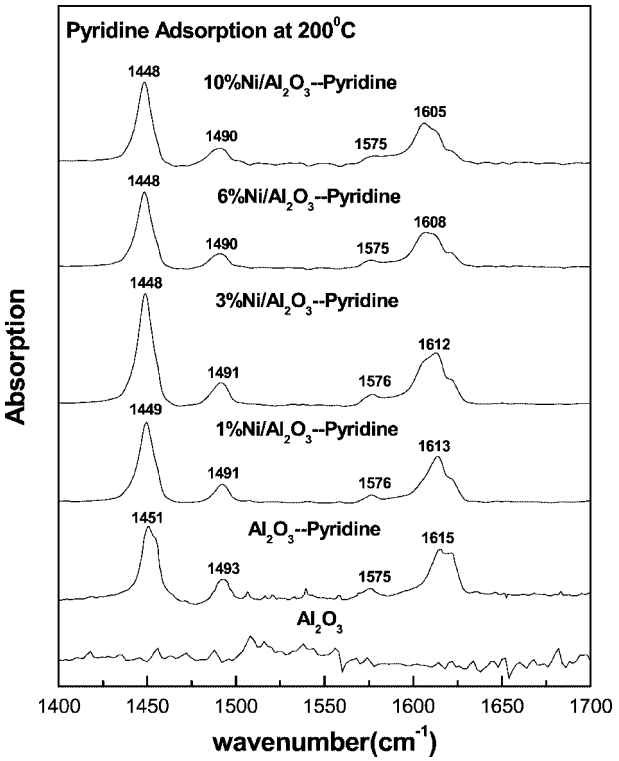

Figure 9. Pyridine adsorption on Ni/Al_2O_3.

to 3 wt% Ni/Al_2O_3 and then decreases. This is due to concurrent and opposite processes: disappearance of Al Lewis sites and creation of Ni Lewis sites. The increase of the surface Lewis acid sites is due to the formation of a surface

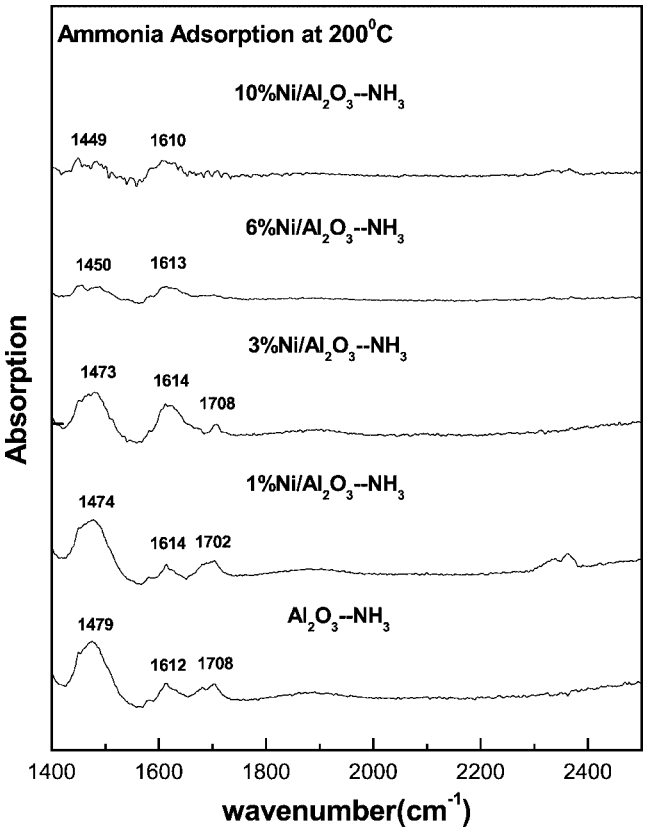

Figure 10. Ammonia adsorption on Ni/Al_2O_3.

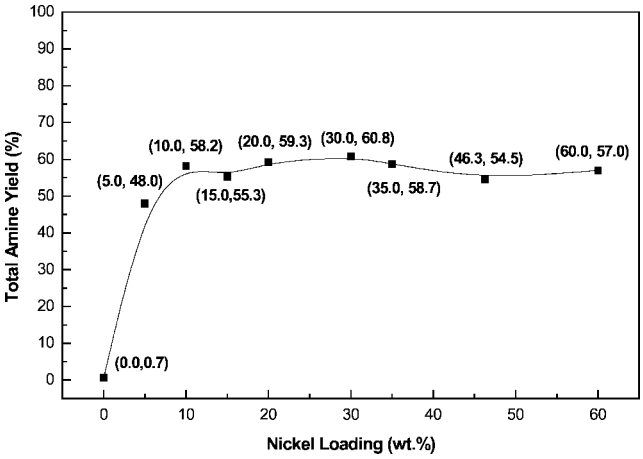

Figure 11. Amination yield of the Ni/Al_2O_3 catalysts.

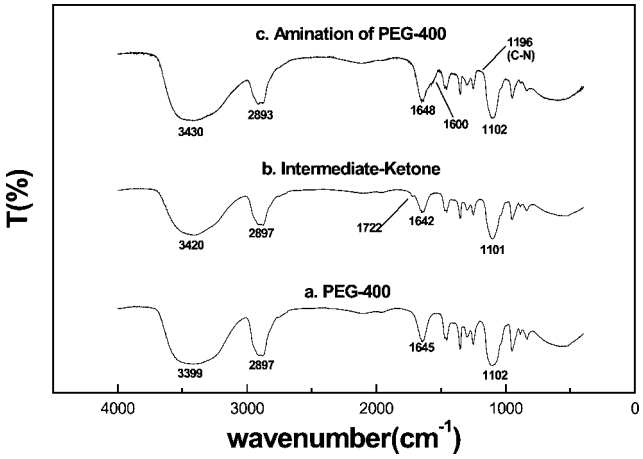

Figure 12. IR studies on amination mechanisms.

nickel overlayer and a surface $NiAl_xO_y$ compound which possesses the coordinatively unsaturated sites to adsorb pyridine molecules. Only the Ni/Al_2O_3 catalysts can adsorb ammonia molecules at 200 °C (figure 10). This is consistent with the IR studies of pyridine adsorption that the PyL band intensity ($\sim$1610 cm^{-1}) increases with nickel loading to 3 wt% Ni/Al_2O_3 and then decreases. The strength of the ammonia adsorption can be the essential factor for controlling the catalytic properties of the amination reaction.

3.5. Amination catalysis

The yield of the amination reaction over the supported nickel catalysts has the following order: Ni/Al_2O_3 > Ni/TiO_2 > Ni/SiO_2. From the above structural investigations, multiple nickel phases such as surface NiO_x species, $NiAl_xO_y$, and NiO are present on the alumina surface, and the ratio of these nickel species is dependent on the nickel loading.

The Ni/Al_2O_3 catalysts with various nickel loading have been further investigated for the amination reaction in order to understand the structure–reactivity relationship. The results have revealed that the amine yield increases with increasing nickel loading up to $\sim$15%, and starts to level off with further increasing nickel loading (figure 11). The trend of amination yield over the Ni/Al_2O_3 catalysts is similar to that of the H_2 consumed of TPR over the same catalysts. Only surface NiO_x species are present on the Ni/Al_2O_3 catalyst with the nickel loading below 15%. Combining the amination catalysis and TPR studies indicates that the surface NiO_x species are the active sites for PEG amination. The amination product has been determined by a titration method in order to decriminate the structure of the amine. The titration results have indicated that the main reaction product is secondary amine instead of primary amine. The formation of the secondary amine product is represented in the model in scheme 1.

One of the OH functional groups in the PEG starts the dehydrogenation and forms the ketone intermediate. The ketone intermediate further reacts with ammonia to form an imine intermediate. The imine intermediate finally reacts with the ketone intermediate to form the observed secondary amine. Upon the presence of excess water in the reactor, the imine intermediate becomes more basic than ammonia and is favored to react with the ketone intermediate. The above amination mechanisms have been further determined by FTIR studies, as shown in figure 12. In the absence of ammonia in the feed, the appearance of the IR band at $\sim$1722 cm^{-1} (figure 12(b)), which is characteristic of the C=O vibrational mode, has revealed that the dehydrogenation of PEG-400 occurs and forms ketone intermediates. The amination of the ketone intermediate to form polyethyleneamine can be

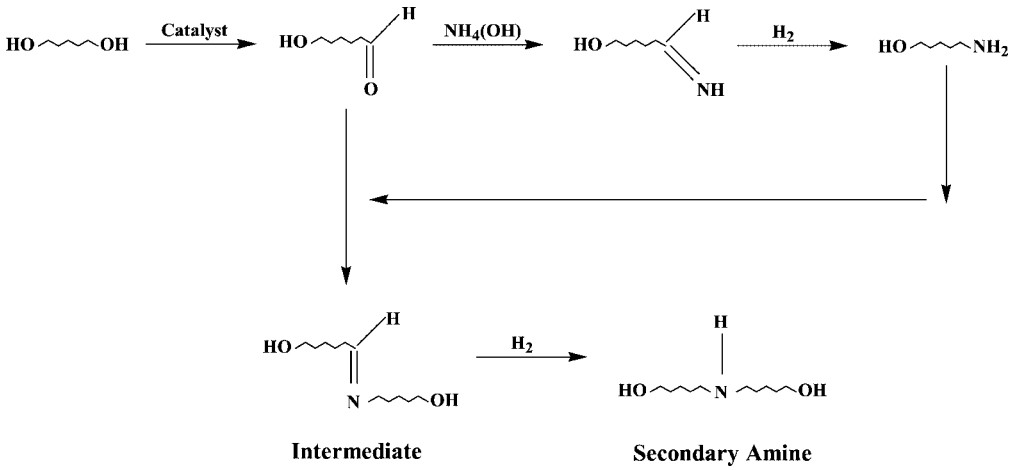

Scheme 1.

further determined by the presence of IR bands at ∼1600 and ∼1196 cm^{-1} characteristic of the vibrational mode of NH_2 and C–N bonds, respectively (figure 12(c)). It is difficult to observe the strong amine stretching bands due to the overlapping of the N–H stretching vibration with the O–H stretching vibration.

4. Conclusions

The formation of nickel-oxide–support interactions in the supported nickel catalysts has a profound effect on the surface structure, reducibility, and surface acidity of these catalysts. A strong metal–support interaction can be applied to molecularly design a catalyst exhibiting high activity and selectivity for the amination process. Supported nickel on Al_2O_3 catalysts consists of surface nickel (NiO_x) species, surface $NiAl_xO_y$ compound, and NiO crystallites. The existence of multiple surface nickel structures enhances the reducibility and surface acidity of the catalysts, and increases the adsorption of pyridine and ammonia molecules. Surface nickel interacts with the titania support to form a surface nickel titanate compound ($NiTiO_x$) which has a lower reducibility. However, the surface Lewis acid sites of the Ni/TiO_2 catalysts increase with increasing nickel loading. The weak interaction between the surface nickel and the silica support results in the formation of nickel oxide crystallites (NiO). Surface acidity of the supported nickel catalysts was determined by the FTIR studies on pyridine and ammonia adsorption. The Ni/Al_2O_3 and Ni/TiO_2 catalysts contain new surface Lewis acid sites and the amount of surface Lewis acid sites increases with increasing nickel loading. Thus, the surface nickel (NiO_x) species present on the Ni/Al_2O_3 catalyst and surface nickel titanate ($NiTiO_x$) compound present on the Ni/TiO_2 catalysts create coordinatively unsaturated sites for adsorbing pyridine. There is no indication of the presence of surface Lewis acid sites on the Ni/SiO_2 catalysts. Furthermore, only the Ni/Al_2O_3 catalysts have shown ammonia adsorption at a temperature of 200 °C.

Reducibility and ammonium adsorption strength of the supported nickel catalysts could be the controlling factor for the amination reaction. Supported nickel on alumina catalysts possess the highest amine yield, and the amine yield increases with increasing nickel loading up to ∼15% and starts to level off with further increasing nickel loading. By comparing amination catalysis with quantitative TPR studies of the H_2 consumed over the Ni/Al_2O_3 catalysts, it appears that the dispersed nickel species are the active sites for amination and the effect of the strong metal–support interaction (SMSI) occurs on the supported nickel catalysts. In addition, the amination product is mainly the secondary amine due to the presence of water.

Acknowledgement

The financial support of the Chinese Petroleum Company of Taiwan (Grant No. NSC-88-CPC-E-005-007) is gratefully acknowledged. The XPS studies provided by the Center of Expansive Instruments at National Tsing Hua University and TPR experiments provided by Professor Israel E. Wachs at Lehigh University are also gratefully acknowledged.

References

[1] H.M. Philip, US Patent 3 152 98 (1964).
[2] L.Y. Ernest, US Patent 3 654 370 (1972).
[3] G.N. Carter and L.Y. Ernest, US Patent 4 075 130 (1978).
[4] W.W. Lewis Jr. and G.W. Harold, US Patent 4 181 682 (1980).
[5] S. Montgomery, *Catalysis of Organic Reactions* (Dekker, New York, 1984) p. 383.
[6] L.J. Czarnecki, C.J. Pereira and W.C. Cheng, in: *15th Organic Reactions Catalysis Society Conference* (Dekker, New York, 1994).
[7] Y. Omoto, K. Iwase and J. Nakamura, Kogyo Kagaku Zasshi 70 (1967) 1508.
[8] K.L. Areshidze and B.S. Tsereteli, *Catalytic Amination of Cyclohexanol* (Inst. Fiz. Org. Khim. Im. Melkishvili, Tbilisi, USSR, 1971).
[9] J. Pasek, P. Koondelik and P. Richter, Ind. Eng. Chem. Prod. Res. Dev. 11 (1972).
[10] S.J. Tauster and S.C. Fung, J. Catal. 55 (1978) 29.
[11] S.J. Tauster, S.C. Fung and R.L. Carten, J. Am. Chem. Soc. 100 (1978) 170.
[12] S.J. Tauster, L.L. Murrell and S.C. Fung, US Patent 4 149 998 (1979).

[13] O.V. Krylov, *Catalysis by Nonmetal Rules for Catalyst Selection* (Academic Press, New York, 1970).
[14] J. Santos, J. Phillips and J.A. Dumesic, J. Catal. 81 (1983) 147.
[15] M.J. Yacaman, Appl. Catal. 13 (1984) 1.
[16] O. Beeck, in: *Advanced Catalysis II*, eds. W.G. Frankenburg, V.I. Komarewsky and E.K. Rideal (Advanced Press, New York, 1950).
[17] B.M.W. Trapnell, *Chemisorption* (Advanced Press, New York, 1955).
[18] H.P. Klug and L.E. Alexander, *X-Ray Diffraction Procedures for Polycrystalline and Amorphous Materials* (Wiley, New York, 1974) p. 618.
[19] H. Winick and S. Doniach, eds., *Synchrotron Radiation Researchs* (Plenum, New York, 1980).
[20] M. Boudart and G. Djéga-Mariadassou, *Kinetics of Heterogeneous Catalytic Reactions* (Masson, Paris, 1982) p. 165.
[21] M.G. Mason, Phys. Rev. B 27 (1983) 748.
[22] W. Eberhardt, P. Fayet, D.M. Cox, Z. Fu, A. Kaldor, R. Sherwood and D. Sondericker, Phys. Rev. Lett. 64 (1990) 780.
[23] F. Solymosi, Catal. Rev. 1 (1967) 233.
[24] G.M. Schwab, Adv. Catal. 27 1 (1978) 1.
[25] H.C. Yao, H.S. Gandhi and M. Shelef, Stud. Surf. Sci. Catal. 11 (1982) 159.
[26] J. Dakta, A.M. Turek, J.M. Jehng and I.E. Wachs, J. Catal. 135 (1992) 186.